A Decentralized Switched System Approach to Overvoltage Prevention in PV Residential Microgrids ⋆

Pulkit Nahata [*,**] **Silvia Mastellone** [**] **Florian Dörfler** [*]

[*] *Automatic Control Lab, Swiss Federal Institute of Technology, 8092 Zurich, Switzerland (e-mail: {pnahata,dorfler}@ethz.ch).*
[**] *Control and Optimization Group, ABB Corporate Research, 5094 Baden, Switzerland (e-mail: silvia.mastellone@ch.abb.com)*

Abstract: In this paper, we consider the problem of overvoltage arising in PV residential microgrids due to excessive power injection into the grid by the PV generators. We propose a decentralized switched controller to curtail excess active power in order to avoid overvoltage while considering the active power constraints. Under different power constraints the system will take different forms: LTI, switched or hybrid system. Convergence to the voltage limit is shown for all three cases.

Keywords: Decentralized control, hybrid systems, solar energy, renewable energy systems

1. INTRODUCTION

Since the past two decades, significant progress has been made in small-scale power generation and energy storage resulting in a reinvigorated interest in the idea of distributed generation. Apart from many advantages such as improved supply security, reduced power transmission losses, and increased standby capacity, the most important advantage lies in its compatibility with renewable sources of energy (Ackermann et al., 2001). With an increasing emphasis on sustainable energy, the recent series of legislations strongly favor the concept of distributed renewable based generation (Taylor et al., 2015).

Solar photovoltaic (PV) based generation is a commonly observed form of distributed generation in low voltage (LV) networks. However, a high PV penetration presents significant technical challenges in distribution networks. A typical household PV system generates more power than required by the load on a clear day and injects most of the generated power into grid. In some LV grids, the installed PV capacity can exceed the peak load by a factor of ten (Appen et al., 2013). The resulting reverse power flow causes a voltage rise in the distribution line. In case of intensive grid connection, this voltage rise may exceed the upper tolerance limit causing an overvoltage. In such a situation, the generating units need to be disconnected to avoid damage to the connected loads. An overvoltage is undesirable and needs to be addressed to ensure power quality.

To address these overvoltage issues, a few engineering approaches are used. A comprehensive overview of these approaches can be found in Tonkoski et al. (2010). One such approach is the curtailment of active power output of PV inverters in case of an overvoltage. We consider LV feeders where resistance/reactance (R/X) ratios are greater than one and can go up to twenty (Eur, 2015). Because of this resistive characteristic, the voltages are more sensitive to active power than reactive power (Yang et al., 2015). This makes the control of PV active power output a more suitable and effective method to mitigate the voltage-rise problem in LV networks.

The existing methods based on active power curtailment (APC) rely either on centralized scheme (Pantziris, 2014), or decentralized schemes (Tonkoski et al., 2011; Yang et al., 2015; Wang et al., 2012) that however exhibit very limited performance. In this work, we aim to design an appropriate decentralized controller that guarantees overvoltage prevention and respects the varying power constraints, i.e., the amount of power that each PV generator is able to provide at any point of time. To capture these varying power constraints, the proposed controller presents switching dynamics. With the switched controller, the resulting closed-loop dynamics show different natures: LTI, switched or hybrid system and depend upon the system operating conditions. The same problem is approached using discrete-time projected optimal control in Nahata et al. (2017)

The paper is organized as follows: Section 2 defines the network model and the overvoltage problem. The core result is presented in Section 3 where the decentralized switched controller is presented and the stability analysis of the closed loop system is shown. For each operating mode and associated closed-loop dynamics, certificate guarantees on closed-loop stability and steady-state voltages are provided. Section 4 presents a case study and finally, Section 5 summarizes the concluding remarks and future work.

Preliminaries and notation: Let $\mathbf{j} = \sqrt{-1}$ be the imaginary unit. Given $x \in \mathbb{R}^n$, let $[x] \in \mathbb{R}^{n\times n}$ be the associated diagonal matrix. $\mathbf{1}_n$ and $\mathbf{0}_n$ are n-dimensional vectors of all ones and zeros. $\mathbb{I}_n$ and $\mathbb{O}_n$ represent identity and zero

⋆ This research was supported by ABB Corporate Research, Switzerland and ETH Zürich.

matrices of dimension $n \times n$. For a given matrix $A \in \mathbb{R}^{n\times n}$ and $\bar{A} \in \mathbb{R}^{n\times n}$ its conjugate, the notation $A > 0$, $A \geq 0$ and $A \succ 0$ and $A \succeq 0$ means that A is positive, non-negative, positive definite, and positive semidefinite respectively. For a real symmetric matrix $A \succeq 0$, $x^T Ax = 0$ if and only if $x \in kernel(A)$ (Van Den Bos, 2007). Given $u, v, w \in \mathbb{R}^n$ with $v_i \leq w_i, i = 1, \cdots, n$, we define the operator $[u]_v^w$ as the component-wise projection of u in the set $\{x \in \mathbb{R}^n : v_i \leq x_i \leq w_i, i = 1, \cdots, n\}$.

2. NETWORK MODELING AND PROBLEM SETUP

2.1 Network Modeling

Standard assumptions enabling positive sequence analysis are made. The residential grid consists of several houses connected to the utility grid via point of common coupling (PCC). We call these individual houses as nodes.

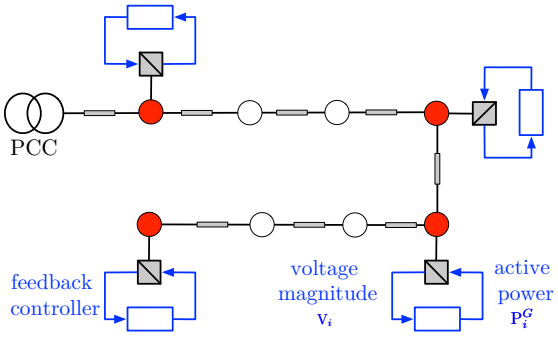

Fig. 1. A typical residential feeder. ● and ○ represent generating and load nodes respectively.

Fig. 1 shows a typical radial feeder with few houses having generation while the others are pure loads. The grid is modeled as a linear circuit represented by a connected weighted graph $O(\mathcal{V}, \mathcal{E}, \mathcal{W})$ where $\mathcal{V} = \{0, \cdots, m+n\}$ is the set of vertices (nodes) and $\mathcal{E} \subseteq \mathcal{V} \times \mathcal{V}$ is the set of edges (branches). The node 0 denotes the PCC. The remaining nodes are classified as : $\mathcal{G} = \{1, \cdots, n\}, n \geq 1$ are the nodes with local generation, and $\mathcal{L} = \{n+1, \cdots, m+n\}, m \geq 1$ are the nodes with pure loads, such that $\mathcal{V} = \mathcal{G} \cup \mathcal{L} \cup \{0\}$. Additionally, we define set $\mathcal{F} = \mathcal{G} \cup \mathcal{L}$.

Let $z_{ij} = r_{ij} + \mathbf{j}x_{ij} \in \mathbb{C}$ be the impedance between node i and j, where $r_{ij} \in \mathbb{R}_{>0}$ is the resistance and $x_{ij} \in \mathbb{R}_{>0}$ is the inductive reactance. The edge weights of the associated graph are the associated admittances $y_{ij} = g_{ij} + \mathbf{j}b_{ij} \in \mathbb{C}$, where $g_{ij} = r_{ij}/(r_{ij}^2 + x_{ij}^2) \in \mathbb{R}_{>0}$ is the associated conductance and $b_{ij} = -x_{ij}/(r_{ij}^2 + x_{ij}^2) \in \mathbb{R}_{<0}$ the susceptance. Owing to high resistances in LV networks, we neglect the shunt reactances in our model. The network is represented by symmetric admittance matrix $Y \in \mathbb{C}^{m+n+1\times m+n+1}$, where the off-diagonal elements are given by $Y_{ij} = Y_{ij} = -y_{ij}$ for each branch $\{i, j\} \in \mathcal{E}$ (0 if $\{i, j\} \notin \mathcal{E}$), and the diagonal elements are given by $Y_{ii} = \sum_{i=0, i\neq j}^{m+n} y_{ij}$. We represent $Y = G + \mathbf{j}B$, where G and B respectively are the conductance and susceptance matrices. Also $G_{ii} = \sum_{i=0, i\neq j}^{m+n} g_{ij} > 0$ and $G_{ij} = -g_{ij} < 0$.

To each node $i \in \mathcal{V}$, we associate a phasor voltage $E_i = V_i e^{\mathbf{j}\theta_i}$ and complex power $S_i = P_i + \mathbf{j}Q_i$. The active power P_i further depends upon the type of node:

$$P_i = \begin{cases} P_i^G + P_i^L & \text{if } i \in \mathcal{G} \\ P_i^L & \text{if } i \in \mathcal{L} \end{cases}$$

where $P_i^G \geq 0$ and $P_i^L \leq 0$ respectively are the active powers generated and consumed at a node. Since the conductors are made of the same material, the R/X exhibits a small variation and is assumed to be constant (Kersting, 2001). We define R/X to be constant, $1/\gamma$, where $0 < \gamma \ll 1$. This implies that $g_{ij}/b_{ij} = -1/\gamma$ and hence, $B = -\gamma G$. The power flow equations are obtained from Kirchhoffs and Ohms laws:

$$S = [E]G\bar{E} - \mathbf{j}[E]B\bar{E} = [E]G\bar{E} + \mathbf{j}\gamma[E]G\bar{E}. \quad (1)$$

These power flow equations are highly non-linear. Since the distribution networks are predominantly resistive in nature, the voltage profile is nearly flat. It is shown in (Bolognani and Dörfler, 2015) that by linearizing the power flow equations around a flat voltage profile (corresponding to a no-load condition of the grid), we obtain:

$$\begin{bmatrix} G & \gamma G \\ \gamma G & -G \end{bmatrix} \begin{bmatrix} V \\ \theta \end{bmatrix} = \begin{bmatrix} P \\ Q \end{bmatrix}, \quad (2)$$

where V and θ are vectors of voltage magnitudes and phase angles. $G \in \mathbb{R}^{m+n+1\times m+n+1}$ is a Laplacian matrix and is positive semidefinite. The node 0 is modeled as a slack bus and its voltage and phase are assumed to be known and constant, $E_0 = V_0 e^{\mathbf{j}0}$. Since V_0 and θ_0 are already known, node 0 can be eliminated from (2). On partitioning (2) into sets $\{0\}$ and $\mathcal{F}$, it can be rewritten as:

$$\begin{bmatrix} G_{00} & G_{0\mathcal{F}} & \gamma G_{00} & \gamma G_{0\mathcal{F}} \\ G_{\mathcal{F}0} & G_{\mathcal{F}\mathcal{F}} & \gamma G_{\mathcal{F}0} & \gamma G_{\mathcal{F}\mathcal{F}} \\ \gamma G_{00} & \gamma G_{0\mathcal{F}} & -G_{00} & -G_{0\mathcal{F}} \\ \gamma G_{\mathcal{F}0} & \gamma G_{\mathcal{F}\mathcal{F}} & -G_{\mathcal{F}0} & -G_{\mathcal{F}\mathcal{F}} \end{bmatrix} \begin{bmatrix} V_0 \\ V_\mathcal{F} \\ \theta_0 \\ \theta_\mathcal{F} \end{bmatrix} = \begin{bmatrix} P_0 \\ P_\mathcal{F} \\ Q_0 \\ Q_\mathcal{F} \end{bmatrix}.$$

$G\mathbf{1}_{m+n+1} = \mathbf{0}_{m+n+1}$ and therefore, $G_{\mathcal{F}0} = -G_{\mathcal{F}\mathcal{F}}\mathbf{1}_{m+n}$. On substituting $\theta_0 = 0$, $P_\mathcal{F}$ and $Q_\mathcal{F}$ are obtained as:

$$-G_{\mathcal{F}\mathcal{F}}\mathbf{1}_{m+n}V_0 + G_{\mathcal{F}\mathcal{F}}V_\mathcal{F} + \gamma G_{\mathcal{F}\mathcal{F}}\theta_\mathcal{F} = P_\mathcal{F} \quad (3a)$$

$$-\gamma G_{\mathcal{F}\mathcal{F}}\mathbf{1}_{m+n}V_0 + \gamma G_{\mathcal{F}\mathcal{F}}V_\mathcal{F} - G_{\mathcal{F}\mathcal{F}}\theta_\mathcal{F} = Q_\mathcal{F}. \quad (3b)$$

Above equations represent power flow without the PCC.

Lemma 1. The matrix $G_{\mathcal{F}\mathcal{F}}$ is irreducible, positive-definite, and Metzler matrix. Its inverse $G_{\mathcal{F}\mathcal{F}}^{-1}$ is well defined, positive, and positive definite (Nahata, 2016).

The invertibility of $G_{\mathcal{F}\mathcal{F}}$ enables us to substitute $\theta_\mathcal{F} = G_{\mathcal{F}\mathcal{F}}^{-1}(-\gamma G_{\mathcal{F}\mathcal{F}}\mathbf{1}_{m+n}V_0 + \gamma G_{\mathcal{F}\mathcal{F}}V_\mathcal{F} - Q_\mathcal{F})$ in (3a). The explicit relationship between $V_\mathcal{F}$ and $P_\mathcal{F}$ can be written as:

$$G_{\mathcal{F}\mathcal{F}}V_\mathcal{F} = \beta P_\mathcal{F} + D, \quad (4)$$

where $\beta = \dfrac{1}{1+\gamma^2}, D = \gamma\beta Q_\mathcal{F} + G_{\mathcal{F}\mathcal{F}}\mathbf{1}_{m+n}V_0$. $Q_\mathcal{F} \in \mathbb{R}^{m+n\times 1}$ represents net reactive power at various nodes and is assumed to be constant. The PV inverters are assumed to operate close to unity power factor and predominantly generate active power.

2.2 Network Reduction

Each generating unit can sense nodal voltage and active power generated. We use network reduction to find an explicit relationship between the sensed parameters and to eliminate the rest. Since $\mathcal{F} = \mathcal{G} \cup \mathcal{L}$, on partitioning $G_{\mathcal{F}\mathcal{F}}$ into $\mathcal{G}$ and $\mathcal{L}$, (4) can be written as:

$$\begin{bmatrix} G_{\mathcal{G}\mathcal{G}} & G_{\mathcal{G}\mathcal{L}} \\ G_{\mathcal{L}\mathcal{G}} & G_{\mathcal{L}\mathcal{L}} \end{bmatrix} \begin{bmatrix} V_\mathcal{G} \\ V_\mathcal{L} \end{bmatrix} = \beta \begin{bmatrix} P_\mathcal{G}^G + P_\mathcal{G}^L \\ P_\mathcal{L}^L \end{bmatrix} + \begin{bmatrix} D_\mathcal{G} \\ D_\mathcal{L} \end{bmatrix}.$$

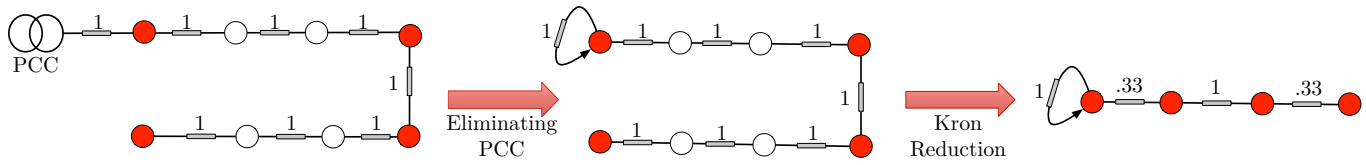

Fig. 2. A representative diagram of network reduction performed on feeder in Fig. 1 with unit conductances.

On the above matrix, we perform Kron reduction (Dörfler and Bullo, 2013) and eliminate $V_{\mathcal{L}}$. On substituting $V_{\mathcal{L}} = -G_{\mathcal{LL}}^{-1}G_{\mathcal{LG}}V_{\mathcal{G}} + \beta G_{\mathcal{LL}}^{-1}P_{\mathcal{L}}^{L} + G_{\mathcal{LL}}^{-1}D_{\mathcal{L}}$ in the upper block, we obtain:

$$V_{\mathcal{G}} = \beta\tilde{G}_{\mathcal{GG}}^{-1}P_{\mathcal{G}}^{G} + D'_{\mathcal{G}}, \tag{5}$$

where $D'_{\mathcal{G}} = \beta P_{\mathcal{G}}^{L} + D_{\mathcal{G}} - \beta G_{\mathcal{GL}}G_{\mathcal{LL}}^{-1}P_{\mathcal{L}}^{L} - G_{\mathcal{GL}}G_{\mathcal{LL}}^{-1}D_{\mathcal{L}}$ and $\tilde{G}_{\mathcal{GG}} = G_{\mathcal{GG}} - G_{\mathcal{GL}}G_{\mathcal{LL}}^{-1}G_{\mathcal{LG}}$. $\tilde{G}_{\mathcal{GG}} = G_{\mathcal{FF}}/G_{\mathcal{LL}}$ is the Schur Complement of $G_{\mathcal{FF}}$ with respect to $G_{\mathcal{LL}}$. The matrix $\tilde{G}_{\mathcal{GG}}$ is irreducible, positive definite, and Metzler as these properties are closed under Schur complementation (Dörfler and Bullo, 2013). Its inverse $\tilde{G}_{\mathcal{GG}}^{-1}$ is well defined, positive and positive definite. A representative diagram of network reduction is shown in Fig. 2.

2.3 The Overvoltage Problem

Definition 2. A node is said to be experiencing overvoltage if its voltage rises beyond a critical voltage V_i^* defined by grid standards.

Remark 3. In (5), the relation between voltage and power is defined by a positive matrix. An increase in active power of a generating node results in rise in voltages at all the nodes in the network.

Lemma 4. (**Overvoltage in radial feeders**). For all net generating nodes in a purely radial feeder, the farthest node from the PCC suffers from maximum overvoltage (Nahata, 2016).

Definition 5. The *critical power* $P_{\mathcal{G}}^{*} \in \mathbb{R}^n$ is the power corresponding to the critical voltage vector V^*. Using (5), the relationship between $P_{\mathcal{G}}^{*}$ and the critical voltage V^* can be expressed as:

$$P_{\mathcal{G}}^{*} = (1/\beta)(\tilde{G}_{\mathcal{GG}}V^* - D'_{\mathcal{G}}). \tag{6}$$

3. DECENTRALIZED SWITCHED INTEGRAL CONTROL

The main aim of an APC based decentralized overvoltage control for PV generators is to inject power until the critical voltage is attained. In this section, we introduce a decentralized feedback based controller to track the critical voltage. However, the power generated by a PV generator is a function of various factors such as cell temperature, shading, inverter efficiency etc. and tracking of critical voltage may not be feasible at all instants. We consider these constraints by means of an additional switching function which switches the controller from one mode to another based upon the voltages of the generating nodes and the varying maximum power output of the inverters.

We define the maximum power that can be injected by a generator at a given instant t in time by a piecewise constant function $\bar{P}_i(t) : [0, \infty) \to \mathbb{R}_{\geq 0}$. Such a function $\bar{P}_i(t)$ has finite number of discontinuities, which we refer as *power switching times*, and takes a constant value between two consecutive power switching times. Two consecutive power switching times define a *power interval*. Since the time scale for PV output variation is of the order of minutes, it is assumed that power intervals are sufficiently long. We assume that $\bar{P}_i(t)$ is continuous from right everywhere: $\bar{P}_i(t) = \lim_{\tau \to t^+} \bar{P}_i(\tau)$ for each $\tau \geq 0$.

Definition 6. A node is said to be saturated if it belongs to the set $\mathcal{S}(t) = \{i \in \mathcal{G} : [P_i^G]_0^{\bar{P}_i(t)} = \bar{P}_i(t) \text{ and } V_i < V_i^*\}$. A node is said to be unsaturated if belongs to set $\mathcal{N}(t) = \mathcal{G} - \mathcal{S}(t)$.

The time dependence of the above sets is sometimes omitted for the simplicity of notation. Ideally, we want all the nodes to be saturated at all time. This is limited by constraints on $\bar{P}_i(t)$. Therefore, an ideal controller should inject maximum power whenever possible and curtail only when necessary. To achieve this goal, we propose the following decentralized switched integral controller:

$$\dot{P}_i^G = m_i u_i (V_i^* - V_i) \qquad i \in \mathcal{G}, \tag{7}$$

where $0 \leq P_i^G \leq \bar{P}_i$, $m_i > 0$ is the droop coefficient and $u_i(P_i^G(t), t)$ is the switching function defined as:

$$u_i(P_i^G(t), t) = \begin{cases} 0 & \text{if } i \in \mathcal{S}(t) \\ 1 & \text{if } i \in \mathcal{N}(t) \end{cases}. \tag{8}$$

The switching function is dependent on both $P_i^G(t)$ and time t. $\bar{P}_i(t)$ and V_i^* partition the state space into operating regions. These operating regions are varying in time as $\bar{P}_i(t)$ is a function of time. Switching can take place when the states hit the boundaries of these operating regions or at a power switching time t when the operating regions change due to a change in $\bar{P}_i(t)$. The change in operating regions in captured by a change in switching function.

We rewrite (7) in vector form as :

$$\dot{P}_{\mathcal{G}}^G = [M][U](V^* - V_{\mathcal{G}}), \tag{9}$$

where $M \in \mathbb{R}^n$ is a vector containing the droop coefficients and $U \in \mathbb{R}^n$ is a vector of switching functions. We assume that the load powers $P_{\mathcal{G}}^L$ and $P_{\mathcal{L}}^L$ are constant. On differentiating (5) with respect to time, we obtain:

$$\tilde{G}_{\mathcal{GG}}\dot{V}_{\mathcal{G}} = \beta\dot{P}_{\mathcal{G}}^G.$$

On substituting $\dot{P}_{\mathcal{G}}^G$ in (9), we obtain the closed-loop switched system as:

$$\dot{V}_{\mathcal{G}}^G = -\beta\tilde{G}_{\mathcal{GG}}^{-1}[M][U](V_{\mathcal{G}} - V^*), \tag{10}$$

where $\tilde{G}_{\mathcal{GG}}^{-1} \succ 0$, $[M] \succ 0$ and $\beta > 0$. Based upon the switching function and operating conditions, the closed-loop dynamics are characterized as:

(1) **Case 1:** $u_i = 1$ $\forall i \in \mathcal{G}$ and $\forall t > 0$, i.e., no active power constraints. The closed-loop system dynamics are linear time invariant (LTI) given as: $\dot{V}_{\mathcal{G}}^G = -\beta\tilde{G}_{\mathcal{GG}}^{-1}[M](V_{\mathcal{G}} - V^*)$.

(2) **Case 2:** u_i is *piece-wise constant* without impulse effects. The lack of impulse effects guarantees continuity of the states. The closed-loop system is represented by the switched dynamics given in (10).
(3) **Case 3:** u_i is *piece-wise constant* with impulse effects. The states jump instantaneously during switching in presence of impulse effects, causing a discontinuity, need to be reinitialized. The closed-loop dynamics in this case are hybrid (Lygeros et al., 2003) and are defined by (10) along with a reset function which reinitializes the system state in case of an impulse.

The various types of power switches are discussed later in section 3.2. We first consider the case of constant maximum power output (no power switching) of all generators and then discuss the general case of varying power outputs of the generators.

3.1 Constant Maximum Power Output

A constant maximum power output implies that $\bar{P}_i$ is continuous and constant for all time. The switching function defined in (8) is only a function of time.

Theorem 7. (**Decentralized switched integral controller under constant maximum power output.**) Consider the switched closed loop system defined by equation (10). For $i \in \mathcal{G}$, the following statements hold true:
1. The system is asymptotically stable and converges to the critical voltage V^* if and only if

$$\bar{P}_i - P_i^G(t) \quad \forall t > 0 \text{ and } \quad \forall i \in G.$$

2. The voltages of the generators are always bounded and are less than or equal to the critical voltage in steady state.

Proof. We will first consider statement 2. At a given time instant t, let the cardinality $\mathcal{S}(t)$ and $\mathcal{N}(t)$ be p and $n-p$ respectively with $P_{\mathcal{S}}^G(t) = \bar{P}_{\mathcal{S}}(t)$ and $P_{\mathcal{N}}^G(t') < \bar{P}_{\mathcal{N}}(t)$. Consider the Lyapunov function:

$$X(V_{\mathcal{G}}) = \frac{1}{2}(V^* - V_{\mathcal{G}})^T \beta^{-1} \tilde{G}_{\mathcal{G}\mathcal{G}}(V^* - V_{\mathcal{G}}).$$

Differentiating the above equation along the trajectory of (10), we obtain:

$$\dot{X}(V_{\mathcal{G}}) = -(V^* - V_{\mathcal{G}})^T [M][U](V^* - V_{\mathcal{G}}).$$

Since $U_{\mathcal{S}} = \mathbf{0}_p$ and $U_{\mathcal{N}} = \mathbf{1}_{n-p}$, $[M][U]$ is positive semi-definite. $\dot{X}$ is negative everywhere, except in the space defined by $V_{\mathcal{S}} \in \mathbb{R}^p$ and $V_{\mathcal{N}} = V_{\mathcal{N}}^*$, where it is zero. The system is stable however, it is not asymptotically stable. The trajectory of the unsaturated nodes will always evolve in the direction such that it minimizes the error $V_{\mathcal{N}}^* - V_{\mathcal{N}}$. Saturated nodes inject maximum power $\bar{P}_{\mathcal{S}}$ and $\dot{P}_{\mathcal{S}}^G = 0$. However, the unsaturated nodes can have $V_{\mathcal{N}}$ greater or less than the critical voltages and $\dot{P}_{\mathcal{N}}^G \neq 0$. The existence of a common Lyapunov function (Liberzon, 2003) guarantees that the voltages are always bounded such that the voltages of unsaturated nodes converge to the critical voltage at steady state.

Let us now consider statement 2. The condition $\bar{P}_i - P_i^G(t^-)\ \forall t > 0,\ \forall i \in G$ implies that generating nodes are always unsaturated and the system never hits the actuation constraints. This is however undesirable as the closed loop system is never able to inject maximum power. In such a scenario, $[U] = \mathbb{I}_n$ and the closed loop system corresponds to a simple linear time invariant system as defined in case 1. All the nodes converge to the critical voltage. ■

3.2 Varying Maximum Power Output

We now consider the case when $\bar{P}_i$ can increase, decrease or stay constant at a power switching time.

Definition 8. For a generating node i and power switching time t, a power switching is said to be positive and negative if $\bar{P}_i(t) - P_i^G(t^-) \geq 0$ and $\bar{P}_i(t) - P_i^G(t^-) < 0$ respectively.

It needs to be ensured that the voltages are within the bounds for all possible switching that can take place in the system. In a given power interval, $\bar{P}_i(t) - P_i^G(t) \geq 0$ holds for all the generating nodes. On a clear day, positive power switching takes place when the maximum power $\bar{P}_i(t)$ increases gradually until it attains a maximum. When $\bar{P}_i(t)$ starts decreasing, a negative power switching occurs. A negative power switching can also take place when $\bar{P}_i(t)$ decreases abruptly on a cloudy day. We will consider the case of positive and negative power switching separately.

Positive Power Switching: We assume that power switching is positive for all the nodes. Thus, $\bar{P}_i(t) - P_i^G(t^-) \geq 0, \forall t$ and $\forall i \in \mathcal{G}$. This condition is important for continuity of states and there are no impulse effects. We will later discuss in Lemma 3.1 that a negative switching at even one of the nodes can result in discontinuity in voltage and power. When such a power switch happens, the switching function may change for few nodes and the closed-loop system will converge to a new equilibrium.

Remark 9. Assuming only positive power switching, if a few other conditions are satisfied, the power injections of the generators do not change. If all the nodes for which a power switching happens at time t satisfy:

$$\bar{P}_i(t^+) = \begin{cases} = \bar{P}_i(t^-) & \text{if } i \in \mathcal{S}(t^-) \\ \geq \bar{P}_i(t^-) & \text{if } i \in \mathcal{N}(t) \end{cases},$$

then $\mathcal{S}(t^+) = \mathcal{S}(t^-)$ and $\mathcal{N}(t^+) = \mathcal{N}(t^-)$. The switching function does not change and the power injections remain unaffected.

Remark 10. (**Strictly positive switching**). The positive power switching is strictly positive if $\bar{P}_i(t) - P_i^G(t^-) > 0$. In such a scenario, $[U] = \mathbb{I}_n\ \forall t > 0$ and hence, the system is time-invariant and all the nodes converge to $V_{\mathcal{G}}^*$.

Negative Power Switching: A negative power switching may occur when there is a decrease in the maximum power output $\bar{P}_i$. A negative power switching at any of the nodes will result in discontinuity in power and voltage. The states need to be reinitialized and a reset function is required. We summarize the properties of a negative power switching in the following Lemma.

Lemma 3.1. For a generating node i, consider a time instant t_1 and negative power switching time t_2 such that $t_1 < t_2$. For $t \in [t_1, t_2)$, if $\bar{P}_i(t_2) - P_i^G(t) < 0$ then the following hold true:
1. Such a switching results in discontinuity in power P_i^G and $V_{\mathcal{G}}$.
2. If the voltages of the generating nodes are bounded in $t \in [t_1, t_2)$, they are also bounded at time $t = t_2$.

Proof. $\bar{P}_i(t_2) < P_i^G(t)$ for $t \in [t_1, t_2)$. At time instant t_2, the maximum power that can be injected is $\bar{P}_i(t_2)$. Therefore, $P_i^G(t_2) = \bar{P}_i(t_2) < P_i^G(t) \leq \bar{P}_i(t_1)$. The left and right limits at t_2 are:

$$P_i(t_2^-) = P_i^G(t) > \bar{P}_i(t_2), \quad P_i(t_2^+) = \bar{P}_i(t_2). \tag{11}$$

Since the limits are not same, there is a discontinuity in power, $\bar{P}_i$. Also, $P_i^G(t) = P_i^G(t_2) + \delta_i(t) = \bar{P}_i(t_2) + \delta_i(t)$, where $\delta_i(t) > 0, t \in [t_1, t_2)$. $V_\mathcal{G}(t)$ can be written as:

$$V_\mathcal{G}(t) = V_\mathcal{G}(t_2) + (\tilde{G}_{\mathcal{GG}}^{-1})_i \delta_i(t).$$

As $\delta(t_2) = 0$ and $\delta(t_2^-) > 0$, $V_\mathcal{G}(t_2) \neq V_\mathcal{G}(t_2^-)$. It can be concluded that a negative switching at any of the nodes results in discontinuity in voltage at all the generating nodes. Also, $\tilde{G}_{\mathcal{GG}}^{-1} > 0$, $V_\mathcal{G}(t_2) < V_\mathcal{G}(t)$. Hence, the voltages are bounded at time $t = t_2$. ■

The closed loop model (10) fails to take into account this discontinuity in power. In case of a negative switching, it is necessary to reinitialize the state. We introduce a hybrid system (Lygeros et al., 2003) model given as:

$$\dot{V}_\mathcal{G}^G = -\beta \tilde{G}_{\mathcal{GG}}^{-1}[M][U](V_\mathcal{G} - V^*) \text{ if } \bar{P}_i(t) - P_i^G(t^-) \geq 0 \tag{12a}$$

$$V_\mathcal{G}(t^+) = \beta \tilde{G}_{\mathcal{GG}}^{-1} \bar{P}(t^+) + D'_\mathcal{G} \text{ if } \bar{P}_i(t) - P_i^G(t^-) < 0. \tag{12b}$$

where (12b) defines the reset function. The above hybrid system is stable and covers cases 1, 2, and 3. During positive power switching, the dynamics are represented solely by (12a). Recall that (12a) corresponds to cases 1, 2 with LTI and switched closed-loop dynamics. Theorem 7 guarantees that the voltages are less than or equal to critical voltages. In case of a negative switching, both (12a) and (12a) define the closed-loop dynamics. Lemma 3.1 guarantees that the voltages will be bounded in the new power interval if they were bounded in the previous interval. Using (5), (6), and (9), (12) can be written solely in terms of $P_\mathcal{G}^G$ as:

$$\dot{P}_\mathcal{G}^G = -\beta[M][U]\tilde{G}_{\mathcal{GG}}^{-1}(P_\mathcal{G}^G - P^*) \text{ if } \bar{P}_i(t) - P_i^G(t^-) \geq 0$$
$$P_\mathcal{G}^G(t^+) = \bar{P}(t^+) \text{ if } \bar{P}_i(t) - P_i^G(t^-) < 0.$$

The system behavior under various possible power switching is consolidated in the following table.

Switching type	System dynamics	Equilibrium voltage
Strictly positive	Linear time invariant	$V_\mathcal{G} = V_\mathcal{G}^*$
Positive	Switched	$V_\mathcal{G} \leq V_\mathcal{G}^*$
Negative	Hybrid	$V_\mathcal{G} \leq V_\mathcal{G}^*$
Mixed	Hybrid	$V_\mathcal{G} \leq V_\mathcal{G}^*$

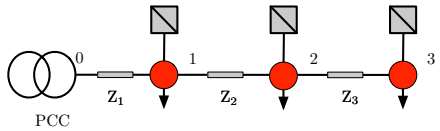

Fig. 3. A radial distribution feeder with three houses.

Example 11. Consider the case of a radial feeder with 3 generating nodes as shown in Fig. 3. We assume that all the houses have same operating conditions and generators of same capacity, and have identical $\bar{P}_i(t)$ $\forall t \geq 0$. In Fig. 4, P_i^* represents the critical power of the respective node. In power interval $[t_1, t_2)$ $\bar{P}_a < P_i^*$, we assume

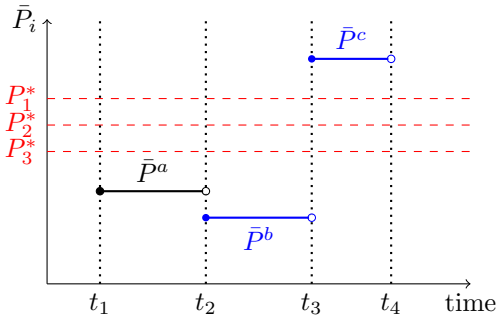

Fig. 4. Variation of maximum power with respect to time

that the controller injects maximum power and all the nodes are saturated, $\dot{P}_i^G = 0$ and $V_i^a < V_i^*$. Now at power switching time t_2, $\bar{P}^b < \bar{P}^a = P_i^G(t_2)$ and all the nodes stay saturated and $V_\mathcal{G}^b < V_\mathcal{G}^a$. Such a switching results in discontinuity in injected power as $P_i^G(t^-) = \bar{P}^a$ and $P_i^G(t^+) = \bar{P}^b$. The crucial case is at power switching time t_3. The controller should inject power only till critical powers are reached and not any further. Theorem 7 guarantees the stability of the closed loop system within the power interval $[t_3, t_4)$.

4. CASE STUDY

In this section, we discuss the performance of the proposed controller in a simulation framework and its effectiveness in mitigating overvoltage problem in LV networks using full nonlinear power flow equations in (1). We consider a test feeder based upon IEEE-13 distribution feeder (Kersting, 2001) as shown in Fig. 5. It is assumed that the infrastructure is symmetric and balanced. The network parameters are adapted to represent an underground residential network and are taken from Tonkoski et al. (2011).

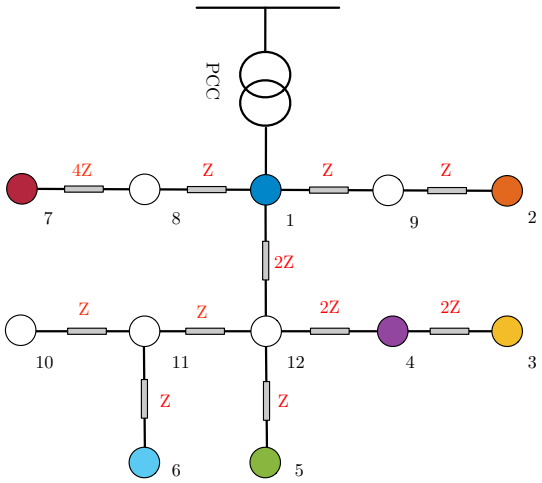

Fig. 5. A residential feeder inspired from IEEE 13 Node test bed.

The critical voltage is chosen as 1.06 p.u. with 1 p.u. as the base voltage. Fig. 6a shows the approximate load and PV profiles on a clear sunny day which are assumed to be identical for all the node. In Fig. 6b, the voltage profile of various generating nodes is shown with and without control. All the generating nodes experience a persistent

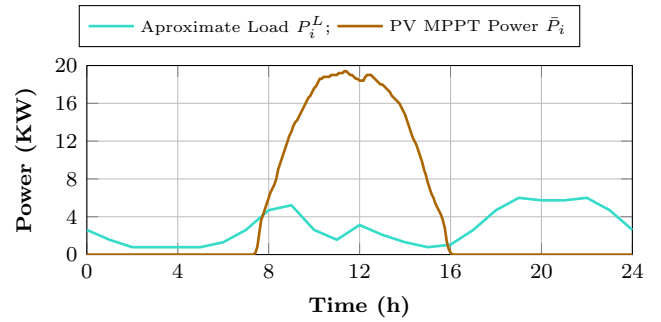

(a) Voltage profiles of various generating nodes.

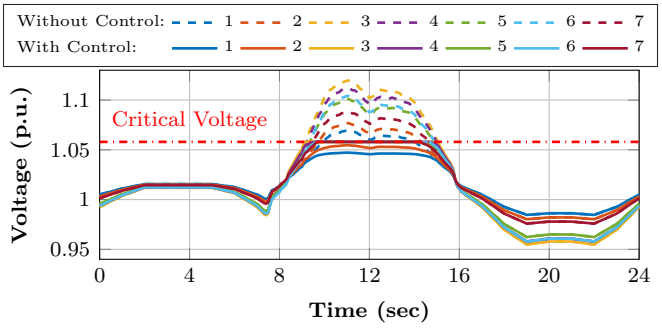

(b) Active power output of PV Generators.

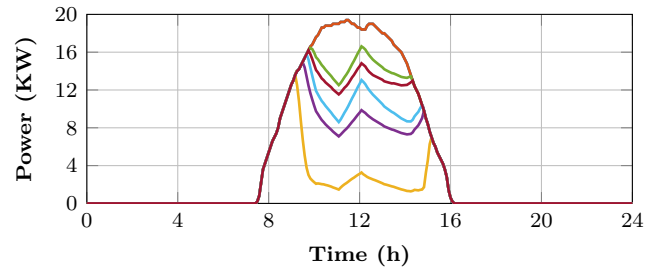

(c) Power flowing through PCC.

Fig. 6. Voltage profiles, nodal generation and power transfer through PCC.

overvoltage throughout the noon during peak generation. Nodes 3 and 4 suffer from maximum overvoltage where as 1 and 2 suffer from the least. In the presence of overvoltage control, the voltages of all the nodes are less than or equal to the critical voltages and an overvoltage is mitigated. Fig. 6c shows the PV power output on clear summer, cloudy summer, and winter days. Node 3 suffers from maximum overvoltage and hence, experiences maximum active power curtailment. Active power is curtailed only in the case of an overvoltage. When the voltages are below critical voltage, the nodes are saturated and inject maximum available power.

5. CONCLUSION

In this paper we presented a switched system approach to address the overvoltage problem in residential PV microgrids. We proposed a modeling framework and a switched control solution, the resulting closed-loop system takes different forms depending on the system status and constraints: 1. LTI system, 2. Switched system, and 3. hybrid system. Each scenario is discussed and stability analysis is presented to guarantee overvoltage prevention, i.e., tracking of the critical voltage while respecting the power constraints. Simulations results are carried out to demonstrate effectiveness of the controller.

REFERENCES

(2015). European Low Voltage Test Feeders. `https://ewh.ieee.org/soc/pes/dsacom/testfeeders`.

Ackermann, T., Andersson, G., and Sder, L. (2001). Distributed generation: a definition. *Electric Power Systems Research*, 57(3), 195 – 204.

Appen, J.V., Braun, M., Stetz, T., Diwold, K., and Geibel, D. (2013). Time in the sun: the challenge of high PV penetration in the german electric grid. *IEEE Power and Energy Magazine*, 11(2), 55–64.

Bolognani, S. and Dörfler, F. (2015). Fast power system analysis via implicit linearization of the power flow manifold. In *Allerton Conference on Communication, Control, and Computing*, 8.

Dörfler, F. and Bullo, F. (2013). Kron reduction of graphs with application to electrical networks. *IEEE Transactions on Circuits ad Systems 1: Regular papers*, 60(1), 150 – 163.

Kersting, W.H. (2001). Radial distribution test feeders. *IEEE Power Engineering Society Winter Meeting*, 2, 908–912.

Liberzon, D. (2003). *Switching in Systems and Control*. Birkhäuser Boston.

Lygeros, J., Johansson, K.H., Simic, S.N., Zhang, J., and Sastry, S.S. (2003). Dynamical properties of hybrid automata. *IEEE Transactions on Automatic Control*, 48(1), 2–17.

Nahata, P. (2016). *Decentralized Active Power Control of PV Inverters in Residential Microgrids*. Master's thesis, ETH Zürich.

Nahata, P., Mastellone, S., and Dörfler, F. (2017). Decentralized optimal projected control of pv inverters in residential microgrids. In *IFAC World Congress*. Submitted.

Pantziris, K. (2014). *Voltage support strategies in a rural low voltage network with high photovoltaic penetration*. Master's thesis, TU Delft.

Taylor, J.A., Dhople, S.V., and Callaway, D.S. (2015). Power systems without fuel. *CoRR*, abs/1506.04799.

Tonkoski, R., Lopes, L.A.C., and EL-Fouly, T.H.M. (2010). Droop-based active power curtailment for overvoltage prevention in grid connected pv inverters. In *2010 IEEE International Symposium on Industrial Electronics*, 2388–2393.

Tonkoski, R., Lopes, L.A.C., and El-Fouly, T.H.M. (2011). Coordinated active power curtailment of grid connected pv inverters for overvoltage prevention. *IEEE Transactions on Sustainable Energy*, 2(2), 139–147.

Van Den Bos, A. (2007). *Parameter Estimation for Scientists and Engineers*. John Wiley and Sons.

Wang, Y., Zhang, P., Li, W., Xiao, W., and Abdollahi, A. (2012). Online overvoltage prevention control of photovoltaic generators in microgrids. *IEEE Transactions on Smart Grid*, 3(4), 2071–2078.

Yang, G., Marra, F., Juamperez, M., Kjær, S., Hashemi, D., Østergaard, J., Ipsen, H., and Frederiksen, H. (2015). Voltage rise mitigation for solar PV integration at LV grids. *Journal of Modern Power Systems and Clean Energy*, 3(3), 411–421.